2005 American Control Conference
June 8-10, 2005. Portland, OR, USA

Microscopic simulations and nonlinear control of dissipative distributed processes*

Antonios Armaou†

Abstract— **A nonlinear continuous-time feedback controller design methodology is developed for distributed processes, whose dynamic behavior can be described by microscopic evolution rules. Employing the micro-Galerkin method to bridge the gap between the microscopic-level evolution rules and the "coarse" process behavior, "coarse" process steady states are estimated and nonlinear process models are identified off-line through the solution of a series of nonlinear programs. Subsequently, nonlinear output feedback controllers are designed, on the basis of the identified process model, that enforce stability in the closed-loop system. The method is used to control a system of coupled nonlinear one-dimensional PDEs (the FitzHugh-Nagumo equations), widely used to describe the formation of patterns in reacting and biological systems. Employing kinetic theory based microscopic realizations of the process, the method is used to design output feedback controllers that stabilize the FHN at an unstable, nonuniform in space, steady state.**

I. Introduction

An important research area that has received a lot of attention in recent years is controller design for distributed processes, mathematically modelled by nonlinear dissipative partial differential equation (PDE) systems. One of the research directions involves the development of methods [1], [2], [3], [4], [5], [6], [7], [8] for controller design based on reduced-order models (e.g., obtained using linear or nonlinear Galerkin's methods) that capture the dominant dynamics of the process and can be solved numerically in real time. An explicit process model is the main prerequisite for the derivation of the reduced-order models, which are used for controller design and real-time implementation.

However, the behavior of an expanding range of distributed processes (for which explicit coarse level mathematical models are unavailable, albeit in principle possible) is being mathematically described using microscopic level simulations (e.g., Lattice Boltzmann (LB), kinetic Monte Carlo (KMC), molecular dynamics (MD)). The lack of an explicit process model precludes the successful use of standard controller design methodologies for distributed parameter systems to such processes.

Motivated by this, linear discrete-time controller design methodologies were recently developed for lumped [9] and distributed [10] processes described by microscopic evolution rules, utilizing the so-called "coarse time-stepper" approach, developed by Kevrekidis and coworkers [11], [12], [13], that circumvents the derivation of the closed form macroscopic PDEs for the process and identifies the essential coarse-scale system behavior. Other model reduction approaches of systems described by microscopic evolution rules include model reduction approaches of the Master Equation [14], the use of wavelets for KMC model reduction [15] and the development of hybrid models for epitaxial growth [16] and crack propagation in materials [17]. In [18], [19], observers based on Monte-Carlo simulations and process measurements were successfully designed to capture the dynamic behavior of microscopic process variables leading to output feedback controller designs. In [20], microscale simulations were employed for the off-line identification of macroscopic process behavior for distributed parameter systems and the derivation of continuous-time observers. Output-feedback controllers were subsequently designed when the manipulated variables entered the system linearly.

This work addresses the issue of *nonlinear continuous-time controller design* to regulate the coarse properties of processes whose dynamic behavior can be described by microscopic evolution rules. Under the assumption that an underlying closed-form process model is, in principle, possible, however unavailable, micro-Galerkin method [12] is employed to bridge the gap between the microscopic-level evolution rules and the "coarse" process behavior and is linked with equation-free methods (such as Recursive Projection Method (RPM) [21]) to obtain estimates of the process stationary states, the slow evolving eigendirections in the neighborhood of the stationary states and a discrete-time reduced-order linear model. Nonlinear continuous-time models are subsequently identified off-line through the *solution of a series of nonlinear programs* employing Carleman linearization [22], [23], and nonlinear output-feedback controllers are subsequently designed using feedback linearization that enforce stability of the target, RPM identified, stationary states in the closed-loop system. The proposed approach is validated on a system of coupled nonlinear one-dimensional PDEs (the FitzHugh-Nagumo equations), widely used to describe the formation of patterns in reacting and biological systems.

II. Process description and preliminaries

The proposed controller design method deals with spatially distributed process systems and hinges on the availability of microscopic/mesoscopic scale simulations that provide information of the process spatiotemporal evolution.

*Financial support for this work from the Pennsylvania State University, Chemical Engineering Department, is gratefully acknowledged.

†Dept. of Chemical Engineering, The Pennsylvania State University, University Park, PA 16802, Tel: (814) 865-5316, Email: armaou@engr.psu.edu

0-7803-9098-9/05/$25.00 ©2005 AACC

Consider, for example, a simplified horizontal flow reactor, where gaseous species A and B flow into the reactor on the left side and a reversible reaction $A+B \rightleftharpoons AB$ takes place, while on the right side, product AB and unreacted species A, B flow out of the reactor. Macroscopic properties of interest include the concentration of the reacting species. Reducing the spatial length-scales to a finer level, we observe that the process involves the motion and collisions of molecules of species A, B and AB. There is a direct link between the number of molecules of each species, their motion characteristics and the collisions between molecules at the "finer" spatial scales and the macroscopic properties of the system at the "coarse" spatial scales of interest. Employing microscopic evolution rules, the behavior of these molecules can be estimated resulting to microscopic/mesoscopic level simulators being produced, such as KMC, MD and LB-based simulators.

Based on microscopic/mesoscopic simulation results, the macroscopic process state variables (e.g., concentrations of species A, B and AB) can be calculated, which will be subsequently used as initial conditions to re-initialized mesoscopic simulations. The calculation of these macroscopic state variables as a function of time can be achieved using "coarse timesteppers" [12], which we employ in the current work and briefly describe for completeness.

The coarse timestepper assumes that an initial condition of the macroscopic state variables is available, as well as microscopic level simulations. The first step in the simulation is called the "lifting" operation, which involves the computation of a number, n, of initial conditions at the microscopic level, conditioned such that their restriction to the macroscopic state variables generate spatial profiles that are equal to the provided macroscopic initial conditions. The second step, termed "evolution" operation, involves the initialization and subsequent evolution of n, microscopic simulations. The third and final step, called "restriction" operation, involves the restriction of the n microscopic simulation results to provide us with the macroscopic state variables, using statistical techniques.

One set of the "lift"-"evolve"-"restrict" operations of the coarse timestepper is the equivalent of one time step using regular time-integrators of systems of nonlinear ordinary differential equation (ODEs). Note that due to the nature of the operations, we can only obtain macroscopic state variable spatial profiles at discrete time instants during the process evolution. The reader may refer to [10], [12] for details on the operation of coarse timesteppers. The coarse timesteppers can be subsequently employed to numerically identify the stationary states of the process. Furthermore, when combined with matrix-free algebra methods, the eigendirections, $\psi_j(z)$ (where z is the spatial coordinate), as well as the associated eigenvalues, μ_j, of the slow-evolving modes of the system can be computed and a linearization of the underlying macroscopic process model in the neighborhood of the identified stationary states can be identified.

Transport-reaction processes are usually characterized by long-term dynamics that can be accurately captured by a few slow-evolving degrees of freedom [24], [2]. Under the assumption that a finite number of slow-evolving modes accurately describes the process dynamics and the rest, infinite, fast-evolving modes are strongly stable and quickly die out, the distributed macroscopic process state variable $\bar{x}(z,t)$ can be approximated by:

$$\bar{x}(z,t) \simeq \sum_{i=1}^{n} x_i(t)\psi_i(z) \tag{1}$$

where $x_i(t) \in \mathbb{R}, \quad i = 1,\ldots,n$ is the i-th modal amplitude, $\psi_i(z), \quad i = 1,\ldots,n$ are the slow system eigendirections identified by matrix-free algebra methods combined with coarse timesteppers. Without loss of generality, we assume that n degrees of freedom are sufficient to accurately describe the long-term dynamics of the process. The central objective of this work is to identify nonlinear dynamic models which accurately describe the evolution of $x_i(t)$ based on information from microscopic simulations. Specifically, we seek to construct nonlinear models of the following form:

$$\begin{aligned} &\dot{x} = f(x) + g(x)u = f(x) + \sum_{j=1}^{m} g_j(x)u_j(t), \\ &x(0) = x_0 \\ &y_m = Sx \\ &y_{ci} = h_i(x), \;\; i = 1,\ldots,m \end{aligned} \tag{2}$$

where $x \in \mathbb{R}^n$ is the state, $u \in \mathbb{R}^m$ is the vector of manipulated variables and $u_j(t)$, is the j-th element of u, $y_m \in \mathbb{R}^q$ is the measured outputs vector, and $y_{ci} \in \mathbb{R}$ is the i-th controlled output. $f(x)$ is a nonlinear vector function of the state, and $g_j(x)$ is a nonlinear vector function which accounts for the influence of the j-th control actuator on the process. $\mathcal{S}$ is the measurement sensor shape function, and $h_i, i = 1,\ldots,m$ is a nonlinear function of the state representing the i-th control objective. Moreover, without loss of generality, we assume that the target steady state of the system is the origin.

In the remainder of this manuscript we need to use the following notation. The Kronecker product between matrices $A \in \mathbb{C}^{N\times M}$ and $B \in \mathbb{C}^{L\times K}$ can be defined as a matrix $C \in \mathbb{C}^{(NL)\times(MK)}$

$$C = A \otimes B \equiv \begin{bmatrix} a_{1,1}B & a_{1,2}B & \cdots & a_{1,M}B \\ a_{2,1}B & a_{2,2}B & \cdots & a_{2,M}B \\ \cdots & \cdots & \cdots & \cdots \\ a_{N,1}B & a_{N,2}B & \cdots & a_{N,M}B \end{bmatrix} \tag{3}$$

We also define the k-th order Kronecker product as $A^{[k]} = A^{[k-1]} \otimes A$, $A^{[1]} = A$ and $A^{[0]} = 1$. $I_n \in \mathbb{R}^{n\times n}$ is defined as the unitary matrix of dimension n. We also define the Lie derivative of the scalar function $h_i(x)$ with respect to the vector function $f(x)$ as $L_f h_i(x) = \dfrac{\partial h_i}{\partial x} f(x)$, $L_f^k h_i(x)$

denotes the k-th order Lie derivative and $L_g L_f^k h_i(x)$ denotes the mixed Lie derivative. Finally, referring to the ODE system of Eq.2, we define the relative degree of the i-th output y_{ci} with respect to the vector of manipulated inputs u as the smallest integer r_i for which:

$$\left[L_{g_1} L_f^{r_i-1} h_i(x) \ \cdots \ L_{g_m} L_f^{r_i-1} h_i(x)\right] \not\equiv [0 \ \cdots \ 0] \quad (4)$$

or $r_i = \infty$ if such an integer does not exist. Furthermore, the matrix:

$$C_0(x) \ = \ \begin{bmatrix} L_{g_1} L_f^{r_1-1} h_1(x) \cdots L_{g_m} L_f^{r_1-1} h_1(x) \\ L_{g_1} L_f^{r_2-1} h_2(x) \cdots L_{g_m} L_f^{r_2-1} h_2(x) \\ \vdots \qquad\qquad \vdots \qquad\qquad \vdots \\ L_{g_1} L_f^{r_l-1} h_m(x) \cdots L_{g_m} L_f^{r_l-1} h_m(x) \end{bmatrix} \quad (5)$$

is the characteristic matrix of the system of Eq.2.

III. Off-line system identification

During the identification stage, the coarse time-steppers through the "lift-evolve-restrict" procedure provide us with a bridge between macroscopic scale system properties and microscopic evolution simulations; initially, the process stationary states are identified (using numerical algebra methods such as recursive projection method [21]) and after variance reduction, a coarse slow discrete-time linearization (i.e. the coarse slow eigenvalues and the corresponding eigenvectors) is derived. Subsequently, the nonlinear dynamic behavior of the process is identified through the solution of a series of dynamic optimization problems. To formulate the dynamic optimization problem as a nonlinear program, we approximate the unidentified system dynamics using polynomial expressions and represent the approximate polynomial system as a linear one through Carleman linearization (linear ODE systems can be solved analytically). We thus formulate a series of nonlinear unconstrained optimization programs, first identifying the open-loop dynamics of the process and subsequently identifying the effect of each control actuator on the system *independently*.

Specifically, the proposed off-line identification of the system, which is achieved in a sequential manner, involves the following steps:

- Use of equation-free Krylov subspace methods, such as Arnoldi process [25], to identify the slow eigenvalues and eigendirections of the process behavior, compute the fast-slow subsystem time-scale separation, and obtain a linearization of the dominant open-loop behavior.
- Identification of the affect of the control actuators on the slow eigenmodes of the system under consideration and computation of a linearization of the actuator effect.
- Generation of $M+1$ ensembles of snapshots during process evolution, employing coarse timesteppers.
  - Use of M_{ol} microscopic simulations to generate an ensemble Y^{ol} of snapshots of the process evolution for a variety of reporting horizons, time-length of simulation and initial conditions for $u_j \equiv 0, \ \forall j = 1, \ldots, m$.
  - Use of M_{cl_j} microscopic simulations to generate m ensembles of Y_j^{cl} of snapshots of the system state during the process evolution for a variety of reporting horizons, time-length of simulation and random manipulated variable piece-wise constant profile of the jth manipulated variable *only*.
- Solution of $M+1$ unconstrained nonlinear programs (NLPs) to identify a *nonlinear* approximation of the slow evolving subsystem.

In the following subsections we present each step in detail.

A. Problem formulation

Referring to the system of Eq.2, we apply McLaurin series expansion to the nonlinear vector fields $f(x)$, $g_j(x)$ in Eq.2 to obtain the equivalent system of the form:

$$\dot{x} = f(x) + g(x)u \equiv \sum_{k=1}^{\infty} A_k x^{[k]} + \sum_{j=1}^{m} \sum_{k=1}^{\infty} B_{j_k} x^{[k]} u_j \quad (6)$$

where $A_k \in \mathbb{C}^{\,n \times (n^k)}$ and $B_{j_k} \in \mathbb{C}^{\,n \times (n^k)}$ are matrices that denote the k-th partial derivatives of $f(x)$ and $g(x)$ with respect to x, respectively, evaluated at $x = 0$. With $x^{[k]}$ we denote the k-th Kronecker product.

We focus on a finite order polynomial approximation of the nonlinear system of order p for $f(x)$ and $p-1$ for $g_j(x)$, respectively, of the form:

$$\dot{x} \simeq \sum_{k=1}^{p} A_k x^{[k]} + \sum_{j=1}^{m} \sum_{k=0}^{p-1} B_{j_k} x^{[k]} u_j \quad (7)$$

To linearize the system of Eq.7, we compute the dynamic behavior of the terms $x^{[k]}$:

$$\frac{d(x^{[k]})}{dt} = \sum_{i=1}^{p-k+1} A_{k,i} x^{[i+k-1]} + \sum_{j=1}^{m} \sum_{i=0}^{p-k} B_{j_{k,i}} x^{[i+k-1]} u_j$$

where $A_{k,i} = \sum_{l=0}^{k-1} I_n^{[l]} \otimes A_i \otimes I_n^{[k-1+l]}$ and $B_{j_{k,i}}$ is defined similarly. Defining $x_{\otimes} = [x^T {x^{[2]}}^T \cdots {x^{[p]}}^T]^T$, the system of Eq.7 can be equivalently written in the following bilinear form:

$$\dot{x}_{\otimes} = \mathcal{A} x_{\otimes} + \sum_{j=1}^{m} \left[\mathcal{B}_j x_{\otimes} u_j + \mathcal{B}_{j_0} u_j\right] \quad (8)$$

where $\mathcal{A}$, $\mathcal{B}_j$ and $\mathcal{B}_{j_0}$ are matrices of appropriate form (the reader may refer to [20] for the form of the matrices). The presented operation, also known as Carleman linearization [22] (previously used for the temporal discretization of ODE systems [23]), presents us with the basis for the identification of the system behavior. The number of unique elements of matrix $\mathcal{A}$ in Eq.8 that need be identified for an order p-th approximation of $f(x)$is $n^2(n^p-1)/(n-1)$, representing the higher order derivatives of $f(x)$. Under appropriate assumptions of smoothness for the unidentified functions $f(x)$ and $g(x)$, the number of parameters to be identified can be drastically reduced (e.g., the number of unidentified

elements of matrix $\mathcal{A}$ becomes $(p+1)(n+p)!/(p+1)!-n!)$. We proceed to compute off-line the unknown parameters of the model.

B. Identification of system linearization

Initially Recursive Projection Method [21] is applied to the process simulator to identify the, possibly unstable, target stationary state of the process and the slow eigendirections in the neighborhood of the stationary state. Due to the nature of RPM and the simulator, discrete-time linearizations of the open-loop process model also become available.

In [10] we presented the derivation of closed-loop linear discrete-time models, which we briefly describe for completeness. The RPM identified model is of the form:

$$x_{sn+1} = Fx_{sn} + Du_n \tag{9}$$

where $x_s \in \mathbb{C}^n$ is a representation of the slow evolving eigendirections of the process of Eq.2, $F \in \mathbb{C}^{n\times n}$ describes their discrete-time linearized dynamics around the stationary-state, $u \in \mathbb{R}^m$ is the vector of the manipulated inputs and $D \in \mathbb{C}^{n\times m}$ approximates the linearized effect of the m control actuators on the slow mode dynamics. The continuous-time behavior of the linearized slow subsystem can be inferred from Eq.9 using the following expressions:

$$\begin{aligned} A_1 &= (1/T)V_F ln(V_F^{-1}FV_F)V_F^{-1}, \\ B_0 &= (F-I)^{-1}A_1 D, \end{aligned} \tag{10}$$

where $B_0 = [B_{10}\ B_{20}\ \cdots\ B_{m0}]$ and T is the reporting horizon of the microscopic simulations.

The reporting horizon of the microscopic scale simulations, T, is an important parameter in the above approach for the identification of the important, slow evolving, spatial patterns, a result of the slaving of the fast dynamics to the dominant ones. Viable reporting horizons are ones that fall in the separation gap between the fast and slow subsystems. We can recursively estimate viable reporting horizons by employing Arnoldi method [26] to estimate the largest eigenvalue of the unidentified fast subsystem, in the neighborhood of the identified by RPM stationary state. If the chosen reporting horizon lies outside this gap, RPM and Arnoldi methods are reinitialized for the new choice of reporting horizon. The reader may refer to [10], [12], [21] for a detailed analysis on the effect of RPM parameters on the identification of the slow subsystem.

C. Identification of open-loop nonlinear behavior

Following the identification of the system linearization, we proceed to the off-line identification of $\mathcal{A}$ and $\mathcal{B}_j$ in a sequential manner. First, M_{ol} microscopic simulations are employed to generate an ensemble Y^{ol} of snapshots of the process evolution for a variety reporting horizons, time-length of simulation and initial conditions for $u_j \equiv 0,\ \forall j = 1,\ldots,m$. Care must be taken so that the reporting horizon of the simulations is large enough, such that it can be ensured that the fast dynamics of the process have become negligible. The snapshots of each different simulation run are used to compute the slow-system modes x and their representation for the Carleman linear form of Eq.8 $x_\otimes$, denoted as $y_{il} \in Y^{ol},\ i = 0,\ldots,n_{f_l},\ l = 1,\ldots M_{ol}$, with T_l the associated reporting horizon, and $n_{f_l}T_l$ the final simulation time. Eq.8 for $u_j \equiv 0,\ \forall j = 1,\ldots,m$ can be solved analytically and the solution is $x_\otimes(t) = exp(\mathcal{A}t)x_\otimes(0)$.

We obtain an estimate of the unknown parameters of $\mathcal{A}$ through the solution of an optimization problem, formulated as an unconstrained *nonlinear optimization program*, which can be subsequently solved using iterative search methods such as SQP and global optimization methods [27], of the form:

$$\begin{aligned} \min_{\mathcal{A}} & \left[\sum_{l=1}^{M_{ol}}\sum_{i=1}^{n_{f_l}}(y_{il}-x_{i,l})^*(y_{il}-x_{i,l})\right],\ y_{il}\in Y^{ol} \\ & \text{s.t.} \\ & x_{i,l} = exp(\mathcal{A}(iT_l))y_{0_l}, \\ & \forall i = 1,\ldots,n_{f_l},\ \ \forall l = 1,\ldots,M_{ol} \end{aligned} \tag{P-I}$$

where the elements of $\mathcal{A}$ representing the higher order derivatives of $f(x)$ in Eq.2 are the free variables. Specifically, the optimization problem is of order $n^2(n^p-n)/(n-1)$, and, under smoothness assumption for $f(x)$, becomes $(p+1)(n+p)!/(p+1)!-(n+1)!$.

D. Identification of actuator effect

Once $\mathcal{A}$ of Eq.8 has been identified we can proceed with the identification of the system response to manipulated input excitation. Furthermore, the effect of each manipulated input can be estimated independently.

Microscopic simulations are employed to generate m ensembles Y_j^{cl} of snapshots of the system during the process evolution for a variety of reporting horizons, time-length of simulation and random manipulated variable profiles $u_j(t) = u_{j_i}(H(iT_l-t)-H(t-(i-1)T_l),\ \forall j = 1,\ldots,m$ ($H(\cdot)$ denotes the Heaviside function) and initial condition at the stationary state ($x_\otimes(0) = 0$). Care must be taken so that the rate of change of the manipulated inputs is constrained so that they do not excite the fast dynamics of the system. The snapshots of each different simulation run are denoted as $y_{il} \in Y_j^{cl},\ i = 0,\ldots,n_{f_l},\ l = 1,\ldots M_{ol}$, with T_l the associated reporting horizon, and $n_{f_l}T_l$ the final simulation time.

The response of the system of Eq.8 to variations of the manipulated input $u_j(t) = u_{j_i}(H(iT_l-t)-H(t-(i-1)T_l)$, with $u_k \equiv 0, \forall k \neq j$ and initial condition at the stationary state, $x_\otimes(0) = 0$, can be derived recursively at each time interval $t \in ((i-1)T_l, iT_l]$, since

$$\dot{x}_\otimes = [\mathcal{A} + \mathcal{B}_j u_{j_i}]x_\otimes + \mathcal{B}_{j_0}u_{j_i}.$$

The above equation can be solved analytically and for $t = iT_l$, $x_{il} \equiv x_\otimes(iT_l)$ it is:

$$\begin{aligned} x_\otimes(iT_l) =& exp([\mathcal{A}+\mathcal{B}_j u_{j_i}]T_l)x_{i-1l} + [\mathcal{A}+\mathcal{B}_j u_{j_i}]^{-1} \\ & \times[exp([\mathcal{A}+\mathcal{B}_j u_{j_i}]T_l) - I]\mathcal{B}_{j_0}u_{j_i}. \end{aligned}$$

Note that $x_{0l} = x_{\otimes}(0) = 0$. We obtain an estimate of the unknown parameters of matrices $\mathcal{B}_j$ through the solution of m unconstrained NLPs. Specifically for the j-th control actuator, the j-th optimization problem has the form:

$$\min_{\mathcal{B}_j} \left[\sum_{l=1}^{M_{cl\,j}} \sum_{i=1}^{n_{f\,l}} (y_{il} - x_{il})^* (y_{il} - x_{il}) \right], \; y_{il} \in Y_j^{cl}$$

s.t.

$$\begin{aligned} x_{il} =& exp([\mathcal{A} + \mathcal{B}_j u_{j_i}] T_l) x_{i-1\,l} \\ &+ [\mathcal{A} + \mathcal{B}_j u_{j_i}]^{-1} [exp([\mathcal{A} + \mathcal{B}_j u_{j_i}] T_l) - I] \mathcal{B}_{j_0} u_{j_i}, \\ & x_{0l} = 0, \\ & \forall i = 1, \ldots, n_{f\,j}, \;\; \forall l = 1, \ldots, M_{cl\,j} \end{aligned} \tag{P-II}$$

IV. Output feedback controller design - Feedback linearization

In this section, we synthesize nonlinear finite-dimensional output feedback controllers to enforce the controlled output of the closed-loop system to follow a prespecified response, provided that the time-scale separation between the slow and the fast subsystems of the unidentified system under investigation is sufficiently large. The output feedback controllers are constructed through combination of state feedback controllers with state observers. To this end, we focus on the approximate system of Eq.7. To simplify our development, we will represent this system in the following compact form:

$$\begin{aligned} \dot{x} &= f(x) + \sum_{j=1}^{m} g_j(x) u_j \\ y_m &= \mathcal{S} x \\ y_{ci} &= h_i(x), \;\; i = 1, \ldots, m \end{aligned} \tag{11}$$

where $f(x) = \sum_{k=1}^{p} A_k x^{[k]}$, $g_j(x) = \sum_{k=0}^{p-1} B_{j\,k} x^{[k]}$, and $\mathcal{S}$ and h have been previously defined in Eq.2. We assume that the relative degree, r_i, in system of Eq.2 is well defined and less than p, for all $i = 1, \ldots, m$.

We use the system of Eq.11 to synthesize nonlinear state feedback controllers of the following general form:

$$u = p(x) + Q(x) v \tag{12}$$

where $p(x)$ is a smooth vector function, $Q(x)$ is a smooth matrix, and $v \in \mathbb{R}^m$ is the constant reference input vector. The synthesis of $[p(x), \;\; Q(x)]$ such that the nonlinear controller of the form of Eq.12 guarantees local exponential stability and forces the output of the system of Eq.11 to follow a desired linear response, is performed by utilizing geometric control methods for nonlinear ODEs (the details of the controller synthesis can be found in [28], and are omitted for brevity; we will only provide with the resulting form of the controller).

Based on relative degree of the system, we assign the following closed-loop behavior to the controlled outputs $y_{ci}(t), \;\; \forall i = 1, \ldots, m$:

$$\sum_{i=1}^{m} \sum_{k=0}^{r_i} \beta_{ik} \frac{d^k y_{ci}}{dt^k} = v \tag{13}$$

where v is the function describing the desired set-points of the controlled outputs. Combining Eq.13 with Eq.11 and assuming that the characteristic matrix of the approximate system of Eq.11, $C_0(x)$ is invertible $\forall\, x \in \mathbb{R}^n$, we derive state feedback controllers of the form:

$$u = \{[\beta_{1r_1} \cdots \beta_{mr_m}] C_0(x)\}^{-1} \left\{ v - \sum_{i=1}^{m} \sum_{k=0}^{r_i} \beta_{ik} L_f^k h_i(x) \right\} \tag{14}$$

Due to the lack of direct measurement of the modal amplitudes $x(t)$ in practice, we assume that there exists an L so that the nonlinear dynamical system:

$$\frac{d\eta}{dt} = f(\eta) + \sum_{j=1}^{m} g_j(\eta) u_j + L[y_m - \mathcal{S}\eta] \tag{15}$$

where η denotes an m-dimensional state vector, is a local exponential observer for the system of Eq.11 (i.e. the discrepancy $|\eta(t) - x(t)|$ tends exponentially to zero).

Finally, it can be shown using Lyapunov-based stability arguments that if the following conditions hold [2]:

1) The roots of the equation:
$$det(F(s)) = 0 \tag{16}$$
where $F(s)$ is an $m \times m$ matrix whose (i,j)-th element is of the form $\sum_{k=0}^{r_i} \beta_{jk}^i s^k$, lie in the open left-half of the complex plane, where β_{jk}^i are adjustable controller parameters.
2) The zero dynamics of the system of Eq.11 are locally exponentially stable.
3) The observer of Eq.15 is locally exponentially stable.

then there exists a positive real number μ, such that if $|x(0)| \leq \mu$, and $\eta(0) = x(0)$, the dynamic output feedback controller:

$$\begin{aligned} \frac{d\eta}{dt} =& f(\eta) + \sum_{j=1}^{m} g_j(\eta) u_j + L[y_m - \mathcal{S}\eta] \\ u \;\; =& \{[\beta_{1r_1} \cdots \beta_{mr_m}] C_0(\eta)\}^{-1} \left\{ v - \sum_{i=1}^{m} \sum_{k=0}^{r_i} \beta_{ik} L_f^k h_i(\eta) \right\} \end{aligned} \tag{17}$$

guarantees local exponential stability and forces the output of the system of Eq.11 to follow a desired linear response. Stability of the closed-loop system (resulting from the application of the controller of Eq.17 to the microscopic simulator) is also achieved, under the condition that the fast dynamics of the process die out sufficiently fast.

V. Application to the FitzHugh-Nagumo equation

The proposed controller design approach is validated using a timestepper of the FitzHugh-Nagumo (FHN) equation, a widely used model of wavy behavior in excitable media in biology [29] and chemistry [11]. The FHN equation has the following closed-form description:

$$\begin{aligned} \frac{\partial v}{\partial t} &= \frac{\partial^2 v}{\partial z^2} + v - w - v^3 + b(z)u(t) \\ \frac{\partial w}{\partial t} &= \delta \frac{\partial^2 w}{\partial z^2} + \epsilon(v - p_1 w - p_0) \\ y_m(t) &= \int_0^L s(z)v(t)dz \end{aligned} \tag{18}$$

subject to the boundary conditions:

$$\frac{\partial v}{\partial z}|_0 = \frac{\partial v}{\partial z}|_L = 0, \quad \frac{\partial w}{\partial z}|_0 = \frac{\partial w}{\partial z}|_L = 0 \tag{19}$$

and the initial conditions:

$$v(0,z) = v_0(z), \quad w(0,z) = x_0(z) \tag{20}$$

where $v(t,z),\ w(t,z) \in \mathbb{R}$ are the system variables, $u(t) \in \mathbb{R}^3$ is the vector of manipulated variables, $y_m(t) \in \mathbb{R}^3$ is the vector of measurements, t is the time, z is the spatial coordinate, $b(z)$ is a row vector describing the distribution function of the control actuators, ϵ, δ, p_1, p_0 are process parameters and L is the length of the spatial domain. We assume that three control actuators are available:

$$b(z) = [g(z, 0.25L)\ \ g(z, 0.50L)\ \ g(z, 0.75L)]$$

where $g(z,\zeta) = exp(-0.3(z-\zeta)^2)$; note that the actuator distribution functions extend over the entire spatial domain of the process. We also assume that three point measurements of $v(t,z)$ are available, of the form:

$$s(z) = [\delta(z - 0.25L)\ \ \delta(z - 0.50L)\ \ \delta(z - 0.75L)]^T$$

where $\delta(\cdot)$ denotes the delta function. In the following simulations, the initial conditions were chosen as $v_0 = 0.5cos(\pi z/L)$ and $w_0 = 0.5cos(\pi z/L)$.

The FHN exhibits multiple steady-state solutions (spatially uniform as well as spatially nonuniform) and spatially nonuniform periodic solutions, depending on the values of the process parameters. For the specific parameter values shown in Table I, the system has at least four spatially nonuniform and three spatially uniform steady-states, presented in Figures 1a and 1b, for v and w respectively.

TABLE I

Process parameters

L	20	δ	4.0	p_1	2.0
T	0.5	ϵ	0.017	p_0	-0.03

Using Galerkin's method with the (analytically derived) eigenfunctions of the spatial operator, we discretize the system in the spatial domain. Linearizing the discretized FHN in the neighborhood of the steady-states and computing the eigenvalues we conclude that the system is locally unstable in the neighborhood of steady states one, two and three, and locally stable in the neighborhood of steady states four, five, six and seven. Furthermore, simulating Eq.18 with $u(t) \equiv 0$ and initial conditions far from the stable steady-states, we observe FHN converges to a locally stable, spatially nonuniform periodic orbit shown in Figures 2a and 2b for $v(t)$ and $w(t)$ respectively. We now focus our attention to steady-state one depicted as thick lines in Figures 1a and 1b for v and w respectively (denoted as $x_{ss,1}$ for the rest of the section). We observe in Table II that there is a finite number of eigenvalues close to the imaginary axis, while an infinite number of them grow towards negative infinity. Moreover we observe that a large spectral gap exists between the second and third eigenvalues ($\epsilon = 0.0108$). This time-scale separation suggests that a few dominant modes may be able to capture the long term dynamics of the open-loop process.

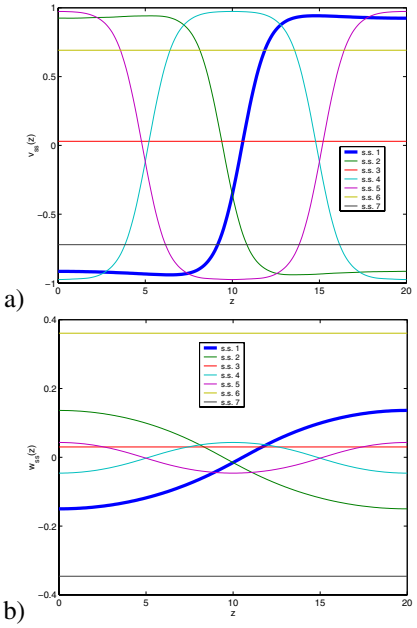

Fig. 1. Open-loop steady states of the FHN equation. (a) v, (b) w.

We now switch to the alternative, kinetic theory based Lattice-Boltzmann-Bhatnagar-Gross-Krook (LB-BGK) scheme [30], which has been constructed so that its zeroth moment fields approximately satisfy the FHN equation [11], [10]. Specifically, we implemented a one-dimensional LB-BGK model [31], [11] to construct a coarse time-stepper with a time-reporting horizon of $T = 0.5$. It combined lifting, from zeroth moment fields to full LB state fields (employing a local equilibrium assumption), LB-BGK "mesoscopic" evolution, and restriction back to zeroth moments corresponding to v and w. The combination of coarse LB-BGK timestepper with RPM located the target coarse stationary state and inferred the coarse stability properties of the process through estimates of the leading coarse eigenvalues/vectors. Through algebraic manipulations, an approximate linear continuous-time coarse slow subsystem in its neighborhood was also computed.

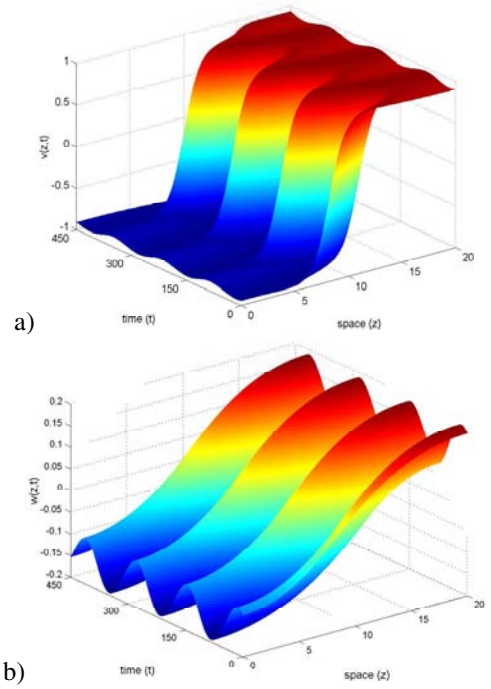

Fig. 2. Open-loop stable periodic orbit of FHN equation. (a) v, (b) w.

Specifically, using as an initial guess the stable coarse stationary profile at $\epsilon = 0.1$ and $\epsilon = 0.11$, we converged to the unstable nonuniform coarse stationary profile at the target value of $\epsilon = 0.017$, which lies beyond the Hopf bifurcation at $\epsilon = 0.019$. We also approximated the coarse slow eigenvalues, their respective eigenvectors and estimated matrix F of Eq.9 for the coarse slow subsystem. Depending on the detailed RPM implementation parameters, and -in particular- on the convergence tolerance, the dimension of the recursively identified coarse slow subspace required to achieve convergence ranged from two to four. The reader may refer to [10], [12], [21] for a detailed analysis on the effect of RPM parameters on the identification of the slow subsystem. In Table II, we present the open-loop eigenvalues of the coarse system and compare with the ones computed based on the FHN discretization. We observe that the eigenvalues computed from RPM are in good agreement with the FHN ones, being within the error tolerance value used by RPM.

TABLE II

EIGENVALUES OF LINEARIZED FHN IN THE NEIGHBORHOOD OF $x_{ss,1}$

Open-loop		Closed-loop
PDE linearization	LB-RPM	LB-Arnoldi
$0.00048 + 0.04665i$	-0.00079+.02492I	-0.01368
$0.00048 - 0.04665i$	-0.00079-.02492I	-0.06947
-0.14428	-0.07289	-0.1272
-0.21245	–	-0.2044
-0.42501	–	-0.4655

Following the coarse open-loop analysis, we computed the coarse process response to actuators' perturbations, and subsequently obtained a linearized expression of their effect on the slow discrete-time subsystem (matrix F of Eq.9). The control objective was defined as the deviation of the slow eigenmodes from their steady-state values:

$$y_{ci} = \int_0^L \begin{bmatrix} \phi_i(z) \\ \psi_i(z) \end{bmatrix}^* \left(\begin{bmatrix} v(z,t) \\ w(z,t) \end{bmatrix} - \begin{bmatrix} v_{ss,1} \\ w_{ss,1} \end{bmatrix} \right) dz,$$
$$i = 1, \ldots, 3$$

where $\phi_i(z)$ and $\psi_i(z)$ are the i-th eigenfunction of $u(z,t)$ and $w(z,t)$, respectively, identified by RPM.

Since two of the identified eigenvalues lie close to the imaginary axis our control objective becomes to place the closed-loop eigenvalues corresponding to the critically stable slow eigenmodes away from the imaginary axis. To retain the time-scale separation between the slow and the fast subsystems (as identified by RPM), the resulting closed-loop eigenvalues should be placed close to the third identified slow eigenvalue. Such an objective will also induce relatively small control actions prescribed by the controller to avoid exciting the fast dynamics of the process. We designed a feedback-linearizing continuous-time controller based on a 3rd order process model with a 3rd-order approximation of the nonlinear behavior, using 1505 snapshots of the process behavior to fit 108 variables. The controller parameters were chosen such that the closed-loop system's eigenvalues remained close to the imaginary axis, in order to preserve the time-scale separation between the fast and slow-subsystems.

In Table II we present the eigenvalues of the closed-loop FHN in the neighborhood of $x_{ss,1}$ and compare them with the eigenvalues of the open-loop system. We observe that the eigenvalues of the closed-loop system are negative implying that the closed loop FHN is stabilized, and the time-scale separation between the slow eigenmodes and the fast ones (gap between the fourth and fifth eigenmodes) persists: spillover did not change the dimension of the closed-loop slow subsystem.

In Figure 3a we present the temporal profiles of the control action. We observe that the control action tends to zero as time progresses, and it achieves stabilizing the FHN process at $x_{ss,1}$ without chattering. The effect of the controller on the dynamics is shown in Figure 3b where the time-profile of the L_2 norm of the FHN converges to the stationary value rapidly and smoothly. In Figure 3c we present the effect of the control action on the deviations of the measurements y_m from their respective values at the target stationary state. We observe that they converge to zero rapidly and without chattering. Figures 4a and 4b present the spatiotemporal profiles of the zeroth moments of the LB-BGK that correspond to $v(z,t)$ and $w(z,t)$, respectively.

REFERENCES

[1] A. Armaou and P. D. Christofides, "Nonlinear feedback control of parabolic PDE systems with time-dependent spatial domains," *J. Math. Anal. Appl.*, vol. 239, pp. 124–157, 1999.

[2] ——, "Finite-dimensional control of nonlinear parabolic PDE systems with time-dependent spatial domains using empirical eigenfunctions," *Int. J. Appl. Math. & Comp. Sci.*, vol. 11, pp. 287–317, 2001.

[3] ——, "Wave suppression by nonlinear finite-dimensional control," *Chem. Eng. Sci.*, vol. 55, pp. 2627–2640, 2000.

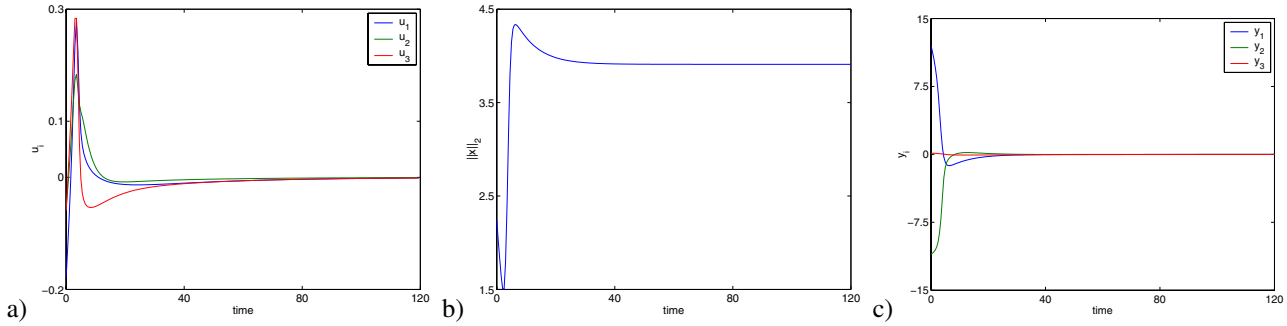

Fig. 3. Time profiles: (a) control action of 3rd order controller (b) L_2 norm of closed-loop FHN under 3rd order controller, (c) deviation of measurements of closed-loop FHN under 3rd order controller from desired values.

[4] J. Baker, A. Armaou, and P. D. Christofides, "Nonlinear control of incompressible fluid flow: Application to Burgers' equation and 2D channel flow," *J. Math. Anal. Appl.*, vol. 252, pp. 230–255, 2000.

[5] P. D. Christofides and P. Daoutidis, "Finite-dimensional control of parabolic PDE systems using approximate inertial manifolds," *J. Math. Anal. Appl.*, vol. 216, pp. 398–420, 1997.

[6] N. El-Farra, A. Armaou, and P. D. Christofides, "Analysis and control of parabolic PDE systems with input constraints," *Automatica*, vol. 39, pp. 715–725, 2003.

[7] P. D. Christofides, *Nonlinear and Robust Control of Partial Differential Equation Systems: Methods and Applications to Transport-Reaction Processes*. New York: Birkhäuser, 2001.

[8] S. Shvartsman and I. G. Kevrekidis, "Nonlinear model reduction for control of distributed systems: a computer-assisted study," *AIChE J.*, vol. 44, pp. 1579–1595, 1998.

[9] C. I. Siettos, A. Armaou, A. G. Makeev, and I. G. Kevrekidis, "Microscopic/stochastic timesteppers and coarse control: a kinetic Monte Carlo example," *AIChE J.*, vol. 49, pp. 1922–1926, 2003.

[10] A. Armaou, C. I. Siettos, and I. G. Kevrekidis, "Time-steppers and 'coarse' control of distributed microscopic processes," *Int. J. Robust & Nonlin. Contr.*, vol. 14, pp. 89–111, 2004.

[11] K. Theodoropoulos, Y.-H. Qian, and I. Kevrekidis, ""Coarse" stability and bifurcation analysis using timesteppers: a reaction diffusion example," *Proc. Natl. Acad. Sci.*, vol. 97, pp. 9840–9843, 2000.

[12] I. G. Kevrekidis, C. W. Gear, J. M. Hyman, P. G. Kevrekidis, O. Runborg, and K. Theodoropoulos, "Equation-free multiscale computation: enabling microscopic simulators to perform system-level tasks," *Comm. Math. Sciences*, vol. 1, pp. 715–762, 2003.

[13] C. I. Siettos, C. C. Pantelides, and I. G. Kevrekidis, "Enabling dynamic process simulators to perform alternative tasks: A time-stepper based toolkit for computer-aided analysis," *Ind. Eng. Chem. Research*, vol. 42, pp. 6795–6801, 2003.

[14] M. A. Gallivan and R. M. Murray, "Reduction and identification methods for Markovian control systems, with application to thin film deposition," *Int. J. Rob. & Nonlin. Con.*, vol. 14, pp. 113–132, 2004.

[15] A. E. Ismail, G. C. Rutledge, and G. Stephanopoulos, "Multiresolution analysis in statistical mechanics. I. Using wavelets to calculate thermodynamic properties," *J. Chem. Phys.*, vol. 118, pp. 4414–4423, 2003.

[16] S. Raimondeau and D. G. Vlachos, "Low-dimensional approximations of multiscale epitaxial growth models for microstructure control of materials," *J. Comp. Phys.*, vol. 160, pp. 564–576, 2000.

[17] J. Q. Broughton, F. F. Abraham, N. Bernstein, and E. Kaxiras, "Concurrent coupling of length scales: Methodology and application," *Phys. Rev. B*, vol. 60, pp. 2391–2403, 1999.

[18] Y. Lou and P. D. Christofides, "Estimation and control of surface roughness in thin film growth using kinetic Monte-Carlo models," *Chem. Eng. Sci.*, vol. 58, pp. 3115–3129, 2003.

[19] ——, "Feedback control of growth rate and surface roughness in thin film growth," *AIChE J.*, vol. 49, pp. 2099–2113, 2003.

[20] A. Armaou, "Continuous-time control of distributed processes via microscopic simulations," in *Proceedings of the American Control Conference*, Boston, Massachusetts, 2004, pp. 933–939.

[21] G. M. Shroff and H. B. Keller, "Stabilization of unstable procedurers: The Recursive Projection Method," *SIAM J. Numer. Anal.*, vol. 30, pp. 1099–1120, 1993.

[22] K. L. Kowalski and W.-H. Steeb, *Nonlinear Dynamical Systems and Carleman Linearization*. Singapore: World Scientific Publishing Company, 1991.

[23] S. A. Svoronos, D. Papageorgiou, and C. Tsiligiannis, "Discretization of nonlinear control-systems via the carleman linearization," *Chem. Eng. Sci.*, vol. 49, pp. 3263–3267, 1994.

[24] R. Temam, *Infinite-Dimensional Dynamical Systems in Mechanics and Physics*. New York: Springer-Verlag, 1988.

[25] C. Kelley, *Iterative Methods for Linear and Nonlinear Equations*, ser. Frontiers in Applied Mathematics. Philadelphia, PA: SIAM, 1995, vol. 16.

[26] K. N. Christodoulou and L. E. Scriven, "Finding leading modes of a viscous free surface flow: An assymetric generalized eigenproblem," *J. Sci. Comp.*, vol. 3, pp. 355–405, 1988.

[27] C. A. Floudas, *Deterministic global optimization: Theory, methods, and applications*, ser. Nonconvex optimization and its applications. Boston, MA: Kluwer Academic, 2000, vol. 37.

[28] A. Isidori, *Nonlinear Control Systems: An Introduction*, 2nd ed. Berlin-Heidelberg: Springer-Verlag, 1989.

[29] J. Keener and J. Sneyd, *Mathematical physiology*. New York: Springer-Verlag, 1998.

[30] S. Succi, *The Lattice Boltzmann Equation for Fluid Dynamics and Beyond*. Oxford, UK: Oxford Science Puplications, 2001.

[31] Y.-H. Qian and S. A. Orszag, "Scalings in diffusion driven reaction $A + B \rightarrow C$ simulations by Lattice BGK models," *J. Stat. Phys.*, vol. 81, pp. 237–253, 1995.

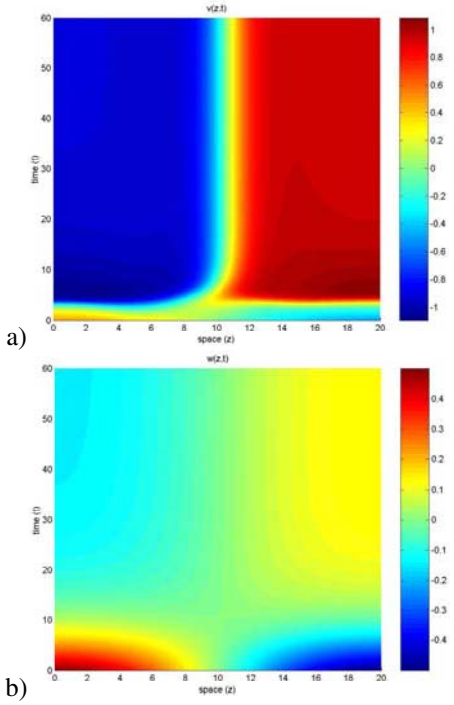

Fig. 4. Closed-loop FHN evolution under 3rd order controller ($v_0 = 0.5cos(\pi z/L)$, $w_0 = 0.5cos(\pi z/L)$). (a) v and (b) w.